



OPEN

Efficient removal of ammonia–nitrogen in wastewater by zeolite molecular sieves prepared from coal fly ash

Qianyang Jiang¹, Jiahuan He¹, Yinwen Wang¹, Bangyao Chen¹, Kewei Tian¹, Keda Yang¹✉, Huangzhao Wei²✉ & Xiaoling Xu¹✉

Zeolite molecular sieves are potential adsorbents for wastewater treatment, characterized by high efficiency, simple process, easy regeneration, and low treatment cost. In this study, zeolite A molecular sieves were prepared using coal fly ash (CFA), which is an effective method for the utilization of CFA. The results showed that the CFA-based zeolite molecular sieves synthesized under optimized conditions exhibited excellent adsorption and removal rates (> 40%) for ammonia–nitrogen in wastewater of different concentrations and properties. The analysis of adsorption kinetics revealed that the adsorption process followed pseudo-second-order kinetics model, indicating that the adsorption of ammonia–nitrogen on zeolite is primarily controlled by chemisorption rather than physisorption. The adsorption process can be divided into two stages, with a higher adsorption rate and a smaller diffusion boundary layer thickness in the first stage, and a lower adsorption rate and an increased diffusion boundary layer thickness in the second stage. This indicates that as the adsorption proceeds, the internal diffusion resistance within the particles gradually increases, leading to a decrease in the adsorption rate until reaching equilibrium, where both the diffusion and adsorption become stable. The adsorption isotherms of ammonia–nitrogen on zeolite A conformed to the assumptions of the Langmuir model, suggesting that the adsorption mechanism primarily involves uniform monolayer adsorption on the surface without intermolecular interactions.

Keywords Zeolite molecular sieves, Coal fly ash, Adsorption, Wastewater treatment, Ammonia–nitrogen

With the continuous development of socio-economic activities, water resource pollution has become increasingly severe, with eutrophication being a particularly prominent issue. Eutrophication of water bodies leads to excessive growth of microorganisms, depleting dissolved oxygen and causing water bodies to turn black, emit foul odors, and trigger harmful algal blooms, becoming a growing global concern¹. Ammonia–nitrogen in wastewater is a significant contributor to eutrophication, with diverse and abundant sources including the use of fertilizers in agriculture, as well as the discharge of domestic wastewater. It is important to note that ammonia–nitrogen not only contributes to eutrophication but also corrodes certain metals and can even pose toxic effects on human health². For example, ammonia is oxidized to nitrite and nitrate by nitrifying bacteria³, and nitrate in drinking water can induce infantile methemoglobinemia⁴. Therefore, effective treatment of ammonia–nitrogen wastewater is of great significance for the prevention and control of eutrophication in water bodies.

Currently, a range of methods have been developed for the removal of ammonia–nitrogen from wastewater, including biological removal methods, chemical treatment methods (breakpoint chlorination, chemical precipitation), and physical treatment methods (stripping, ion exchange adsorption)⁵. However, these methods also have limitations. For example, biological removal methods are susceptible to environmental conditions, have slow reaction rates, long reaction times, require large working areas, and have limited practical applications. Chemical treatment methods can generate secondary pollution and consume a large amount of chemicals. The high cost of chemicals restricts the large-scale application of this method. Additionally, the physical treatment method of stripping is greatly affected by temperature and cannot be widely applied. Ion exchange adsorption, represented

¹Key Laboratory of Artificial Organs and Computational Medicine in Zhejiang Province, Shulan International Medical College, Zhejiang Shuren University, Hangzhou 310015, People's Republic of China. ²Dalian Institute of Chemical Physics, Chinese Academy of Sciences, Dalian 116023, People's Republic of China. ✉email: kdyang@zjsru.edu.cn; whzhdicpwtg@dicp.ac.cn; ziyao1988@zju.edu.cn

by ion exchange resins, has received increasing research attention due to its low cost, high ammonia–nitrogen removal efficiency, and convenient operation and regeneration methods⁶. However, adsorbents such as ion exchange resins have limited capacity for adsorbing ammonia–nitrogen. When treating high-concentration ammonia–nitrogen wastewater, more ion exchange resins may be required or resin recovery and regeneration may need to be performed more frequently, increasing operational costs and complexity⁷.

Zeolite, as an inorganic material, exhibits high stability. It not only shows excellent performance in the low-carbon treatment of wastewater from ammonia nitrogen production, such as adsorption of ammonia nitrogen⁸, removal of nitrate⁹. Park et al.⁹ utilized the active metal sites provided by the zeolite surface to enhance the performance of palladium (Pd) and tin (Sn) bimetallic catalysts, thereby enhancing the denitrification process, achieving efficient removal of nitrate from water bodies. Sama M. et al.¹⁰ innovatively utilized ash extracted from aquatic reeds as a cost-effective and efficient source of silica for the synthesis of zeolite molecular sieves. This approach offers a novel perspective on the raw materials used for zeolite synthesis. Additionally, zeolites have shown enormous potential in the field of medical wastewater treatment (such as adsorption of antibiotics)^{11–14}.

However, zeolite molecular sieves also face challenges such as high material preparation costs and a lack of large-scale promotion¹⁵. Although zeolite molecular sieves prepared from CFA can effectively address the cost issue¹⁶, there is still a lack of systematic research on the influence of different preparation conditions on the adsorption capacity of zeolite molecular sieves.

In order to enhance the capability of CFA-based zeolite molecular sieves in treating ammonia–nitrogen wastewater, this study focuses on investigating the influence of raw material ratios and preparation conditions of CFA-based zeolite molecular sieves on the adsorption capacity of ammonia–nitrogen in wastewater, and selects the optimal conditions for preparing CFA-based zeolite molecular sieves using alkali fusion hydrothermal method¹⁷. Furthermore, the adsorption rates and removal efficiencies of zeolite molecular sieves in ammonia–nitrogen wastewater of different concentrations and properties are systematically tested, and the adsorption kinetics are studied.

Materials and methods

Materials

The raw CFA is from Zhejiang University of Technology, and its main components are shown in Table 1. SiO₂ and Al₂O₃ are its main components, accounting for more than 80% of the total mass. They provide abundant sources of silicon and aluminum for the synthesis of zeolite, making it an inexpensive material for the preparation of zeolite molecular sieves¹⁸. Sodium hydroxide (pellets, AR) and hydrochloric acid (36.0–38.0%) were purchased from Sinopharm Chemical Reagent Co., Ltd.; magnesium chloride (99%, AR), ammonium chloride (99.5%, AR), and Nessler's reagent were obtained from Shanghai Aladdin Biochemical Technology Co., Ltd.; calcium chloride (96%, AR) was sourced from Shanghai Yuanye Biotechnology Co., Ltd. Deionized water was used throughout the experiments.

Preparation of CFA-based molecular sieves

Preprocessing of CFA

The preparation process of CFA-based zeolite molecular sieves is as follows. A certain amount of raw CFA is ground and sequentially sieved using different standard sieves with pore sizes of 50 mesh, 100 mesh, 150 mesh, and 200 mesh. The sieved CFA is then directly placed in a muffle furnace and calcined at a high temperature of 750 °C for 2 h to remove carbon. After cooling to room temperature, the calcined CFA is mixed with hydrochloric acid solution in a ratio of 1:20 (mass of CFA to volume of hydrochloric acid solution with a mass fraction of 5.0%; 5.0% hydrochloric acid using 36% concentrated hydrochloric acid). The mixture is stirred and heated for 2 h. After the reaction is complete, deionized water is added and continuous filtration and washing are performed until neutral. The filter residue is dried to obtain the preprocessed CFA.

Preparation of CFA-based zeolite molecular sieves under different conditions

Taking the preprocessed CFA, the experimental flow chart of zeolite A synthesis is shown in Fig. 1. The optimal factors for preparing zeolite molecular sieves can be explored by controlling three variables: temperature, alkali-to-ash ratio, and solid-to-liquid ratio. The conditions are as follows:

1. Under the conditions of calcination temperature of 750 °C, calcination time of 120 min, solid-to-liquid ratio of 1:6, hydrothermal temperature of 75 °C, and hydrothermal time of 6 h, NaOH/CFA mass ratio 1(D1), 1.2(D2), 1.4 (D3) and 1.6 (D4).
2. Under the condition of NaOH/CFA mass ratio 1.2, calcination time of 120 min, solid-to-liquid ratio of 1:6, hydrothermal temperature of 75 °C, and hydrothermal time of 6 h, the calcination temperatures are set as 600 °C (E1), 700 °C (E2), 750 °C (D2) and 800 °C (E3).

	SiO ₂	Al ₂ O ₃	Fe ₂ O ₃	CaO	TiO ₂	MgO	Na ₂ O	K ₂ O	SO ₃	LOI	total
CFA (wt.%)	48.21	33.18	4.80	5.68	1.61	0.75	0.45	0.29	0.26	1.20	96.44

Table 1. Chemical constituent of raw CFA. LOI ignition loss, 950 °C.

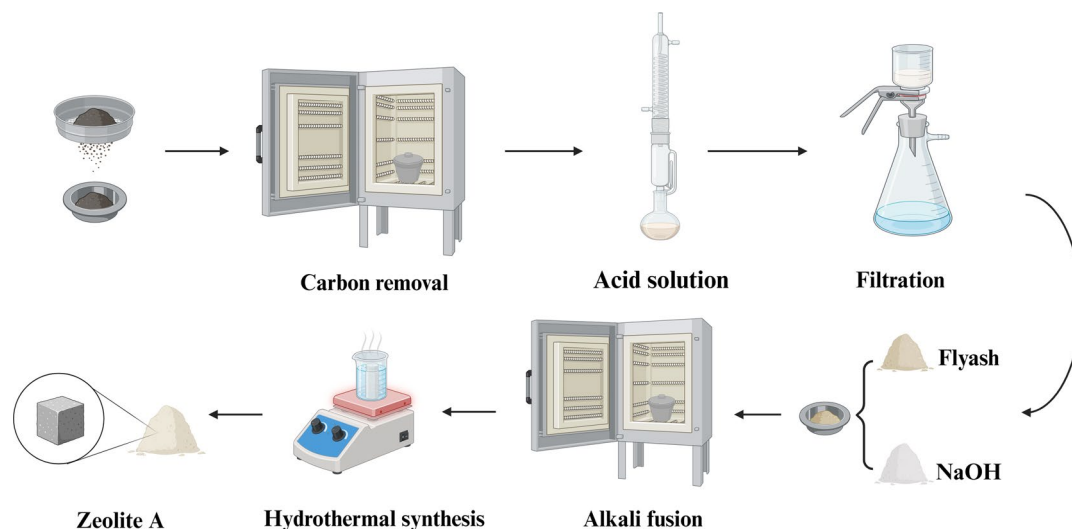


Fig. 1. Experimental flow chart of zeolite A synthesis.

- Under the condition of NaOH/CFA mass ratio 1.2 and the conditions of calcination temperature of 750 °C, calcination time of 120 min, hydrothermal temperature of 75 °C, and hydrothermal time of 6 h, the solid-to-liquid ratios are set as 1:5 (F1), 1:6 (D2), 1:7 (F2), and 1:8 (F3).

Characterization of molecular sieves

Characterization of molecular sieves involves various techniques. The crystal structure was characterized by X-ray diffraction (XRD) using a Bruker D8 ADVANCE X-ray diffractometer. The pore size and arrangement was characterized by transmission electron microscopy (TEM) using a JEOL JEM-1400 TEM. Scanning electron microscopy (SEM) analysis of the composition, morphology, and structure of the sample surface is carried out using a ZEISS GEMINI 300 SEM. Additionally, particle size and surface potential measurements are performed using a particle size and surface potential analyzer (NS-90), and the specific surface area of zeolite was measured using a Surface Area Analyzer (AUTOSORB-IQ2-MP).

Adsorption performance of ammonia–nitrogen in wastewater

The adsorption capacity of zeolite for ammonia–nitrogen was determined using the nanoscale reagent spectrophotometric method. A standard solution of ammonia–nitrogen with a concentration of 100 mg/L was used as the adsorbate. The solution was then diluted in half to prepare standard solutions with concentrations of 1.5626 mg/L, 3.125 mg/L, 6.25 mg/L, 12.5 mg/L, and 25 mg/L of ammonia–nitrogen. 1 mL of the nanoscale reagent was added to each solution. The absorbance was measured at a wavelength of 420 nm using an enzyme-linked immunosorbent assay (ELISA) reader, with water as the reference. The absorbance of the blank solution was subtracted from the corrected absorbance obtained from the measurements. The experiment was performed in triplicate, and the average value was taken. The resulting standard curve equation was $y = 0.0624x + 0.0147$.

After obtaining the standard curve equation, 0.05 g of zeolite A molecular sieve was taken and mixed with 100 ml of ammonium chloride solution at 25 °C. The mixture was then shaken at 260 rpm for 70 min. The upper clear liquid was extracted using a syringe, and the filtrate was quantitatively extracted, diluted, and mixed with a color reagent. After thorough mixing, the absorbance of the solution was measured at a wavelength of 420 nm using a spectrophotometer. The concentration of ammonia–nitrogen in the solution was calculated using the linear regression equation obtained from the standard curve. Finally, the adsorption capacity of ammonia–nitrogen by zeolite was determined by subtracting the calculated ammonia–nitrogen content in the solution from the initial concentration of ammonia–nitrogen.

The formulas for ammonia–nitrogen removal efficiency¹⁹ and adsorption capacity²⁰ are shown as (1) and (2) respectively:

$$\theta = \frac{C_0 - C_1}{C_0} \times 100\% \quad (1)$$

$$q = \frac{(C_0 - C_1) \times V}{m} \quad (2)$$

where θ represents the ammonia–nitrogen removal efficiency, C_0 is the initial concentration of ammonia–nitrogen in the solution in mg/L, C_1 is the concentration of ammonia–nitrogen in the solution after adsorption in mg/L, q is the adsorption capacity in mg/g, V is the volume of the solution in L, and m is the mass of zeolite in mg.

The effect of adsorption time on ammonia–nitrogen adsorption efficiency

Under room temperature conditions, 50 ml of ammonia–nitrogen solution with a concentration of 100 mg/L was added to 6 numbered centrifuge tubes of 50 ml each. Then, 0.05 g of CFA zeolite was added to each tube, and the tubes were oscillated at 260 rpm on a multi-purpose shaker for 5 min, 10 min, 20 min, 30 min, 50 min, and 70 min. After centrifugation at 7000 rpm, the concentration of ammonia–nitrogen in the supernatant was measured using a spectrophotometric method. The ammonia–nitrogen removal efficiency was calculated, and the experiment was conducted in triplicate.

The effect of initial solution concentration on ammonia–nitrogen adsorption efficiency

At room temperature, an ammonia nitrogen solution of 60 mg/L, 80 mg/L, 100 mg/L, 150 mg/L, and 200 mg/L was prepared. Then, 50 ml of each diluted solution was added to 5 numbered centrifuge tubes of 50 ml each. Subsequently, 0.05 g of CFA zeolite was added to each tube, and the tubes were oscillated at 260 rpm on a multi-purpose shaker for 70 min. After centrifugation at 7000 rpm, the concentration of ammonia–nitrogen in the supernatant was measured using a spectrophotometric method. The ammonia–nitrogen removal efficiency was calculated, and the experiment was conducted in triplicate.

The effect of temperature on ammonia–nitrogen adsorption efficiency

Under conditions of 25 °C, 30 °C, 35 °C, 40 °C, and 45 °C, 50 ml of ammonia–nitrogen solution with a concentration of 100 mg/L was added to 5 numbered centrifuge tubes of 50 ml each. Then, 0.05 g of CFA zeolite was added to each tube. The tubes were oscillated at 260 rpm on a multi-purpose shaker for 70 min. After centrifugation at 7000 rpm, the concentration of ammonia–nitrogen in the supernatant was measured using a spectrophotometric method. The ammonia–nitrogen removal efficiency was calculated, and the experiment was conducted in triplicate.

The effect of solution pH on ammonia–nitrogen adsorption efficiency

Under room temperature conditions, the ammonia–nitrogen solution with a concentration of 100 mg/L was adjusted to pH 5, 6, 7, 8, and 9 using HCl and NaOH solutions. Then, 50 ml of each adjusted solution was added to 5 numbered centrifuge tubes of 50 ml each. Subsequently, 0.05 g of CFA zeolite was added to each tube, and the tubes were oscillated at 260 rpm on a multi-purpose shaker for 70 min. After centrifugation at 7000 rpm, the concentration of ammonia–nitrogen in the supernatant was measured using a spectrophotometric method. The ammonia–nitrogen removal efficiency was calculated, and the experiment was conducted in triplicate.

The effect of competing cations on ammonia–nitrogen adsorption efficiency

Under room temperature conditions, 25 ml of simulated water sample with an ammonia–nitrogen concentration of 200 mg/L was added to 2 numbered centrifuge tubes of 50 ml each. Then, 25 ml of 200 mg/L magnesium chloride solution and calcium chloride solution were added to each tube. Subsequently, 0.05 g of CFA zeolite was added to each tube, and the tubes were oscillated at 260 rpm on a multi-purpose shaker for 70 min. After centrifugation at 7000 rpm, the concentration of ammonia–nitrogen in the supernatant was measured using a spectrophotometric method. The ammonia–nitrogen removal efficiency was calculated, and the experiment was conducted in triplicate.

Regeneration of zeolite previously adsorbed with ammonia nitrogen and evaluation of its ammonia nitrogen re-removal capacity

To regenerate the zeolite that has already adsorbed ammonia nitrogen, first rinse it with water three times, then centrifuge and place the sediment in an oven to dry. Subsequently, add the dried zeolite to a 4% NaOH solution at a solid-to-liquid ratio of 500 g/L, and agitate the mixture at 25 °C for 5 h. After agitation, rinse the zeolite with water again and dry it to obtain the regenerated zeolite.

To evaluate the ammonia nitrogen removal capacity of the regenerated zeolite, take 0.05 g of the regenerated zeolite and perform an adsorption test under the conditions of 25 °C, an initial ammonia nitrogen concentration of 100 mg/L, pH 7, and an adsorption time of 70 min. Calculate the adsorption capacity using the OD value. Utilize Origin 2021 software to plot a bar graph comparing the initial and subsequent adsorption capacities.

Zeolite molecular sieve adsorption kinetics analysis*Adsorption kinetic model*

The study of adsorption kinetics involves investigating the rate at which substances are transferred and the changes in equilibrium concentration over time during the adsorption process. By analyzing the interactions between the adsorbent and the adsorbate, as well as the mass transfer process, it is possible to understand the influence of factors such as intermolecular forces and diffusion rates on the adsorption behavior. Therefore, the study of adsorption kinetics is crucial for understanding the adsorption mechanism. Typically, kinetic equations are used to describe the adsorption kinetics process. The pseudo-first-order kinetic model and the pseudo-second-order kinetic model correspond to Eqs. (3) and (4), respectively.

$$\ln(q_e - q_t) = \ln q_e - k_1 t \quad (3)$$

$$\frac{t}{q_t} = \frac{t}{q_e} + \frac{1}{k_2 q_e^2} \quad (4)$$

where q_t represents the adsorption capacity at any given time (mg/g), q_e represents the adsorption capacity at equilibrium (mg/g), k_1 and k_2 are the rate constants for the pseudo-first-order and pseudo-second-order kinetic equations, respectively (min^{-1}), and t represents the reaction time (min).

The pseudo-first-order kinetic model is typically used to describe the initial stage of a reaction, when the adsorbate concentration is low and the adsorption rate is fast. However, as the adsorbate concentration increases, the adsorption rate gradually slows down. In such cases, the pseudo-first-order kinetic model cannot accurately describe the entire adsorption reaction process. On the other hand, the pseudo-second-order kinetic model incorporates surface adsorption and internal diffusion processes, allowing for a better description of the overall adsorption reaction²¹.

Internal particle diffusion model

In order to elucidate the influence of internal diffusion on the adsorption rate and capacity during the adsorption process and gain a deeper understanding of the diffusion kinetics within the particles, we conducted an analysis using an intra-particle diffusion model on the kinetic data. The intra-particle diffusion model is a mathematical model used to describe the phenomenon of internal diffusion within particles. It helps us to reveal the impact of internal diffusion on the adsorption rate and capacity during the adsorption process. The diffusion kinetics equation²² of the intra-particle diffusion model is given by Eq. (5):

$$q_t = Kt^{0.5} + C \quad (5)$$

where q_t is the amount of adsorbate adsorbed at time t , K is the intra-particle diffusion rate constant, t is the time, and C is the thickness of the boundary layer.

Adsorption isotherm model

In order to further study the surface adsorption process, we used the adsorption isotherm models to investigate the interaction between the adsorbent and the adsorbate. Langmuir and Freundlich are two common adsorption isotherm models that can be used to analyze the adsorption characteristics of ammonia–nitrogen on A-type molecular sieves²³. The Langmuir model assumes that the adsorbent surface has uniform adsorption sites and no interaction between the adsorption sites²⁴. Based on this assumption, the Langmuir model can predict the maximum adsorption capacity during monolayer adsorption. The Freundlich model is an empirical formula widely used to describe adsorption phenomena. It can explain the adsorption behavior of the adsorbent on non-uniform surfaces with different binding energies. By using a mathematical expression to describe the interaction between the adsorbent and the adsorbate, the Freundlich model can predict the shape and characteristics of the adsorption isotherm. The adsorption characteristics of ammonia–nitrogen on Zeolite A molecular sieves are described by the Langmuir^{25–27} and Freundlich^{28,29} isotherm models as shown in Eqs. (6) and (7):

$$\frac{C_e}{q_e} = \frac{1}{q_m k_L} + \frac{C_e}{q_m} \quad (6)$$

$$\ln q_e = \ln k_F + \frac{1}{n} \ln C_e \quad (7)$$

where, q_e and q_m ($\text{mg} \cdot \text{g}^{-1}$) are the equilibrium adsorption capacity and theoretical saturation adsorption capacity of ammonia–nitrogen; C_e ($\text{mg} \cdot \text{L}^{-1}$) is the equilibrium concentration of MB; k_L ($\text{m}^3 \cdot \text{g}^{-1}$) is the Langmuir constant, and k_F ($\text{mg} \cdot \text{g}^{-1} (\text{m}^3 \cdot \text{mg}^{-1})^{1/n}$) and n are the Freundlich constants.

Results and discussion

Selection of preparation conditions for CFA molecular sieve

NaOH/CFA mass ratio

Figure 2A shows the XRD pattern of samples obtained under different NaOH/CFA mass ratios, compared with the powder diffraction file (PDF) cards in the standard database. The characteristic peaks of NaA zeolite (PDF 39-02223) are observed, indicating that the prepared molecular sieve is of the Zeolite A, with the molecular formula $\text{Na}_2\text{O} \cdot \text{Al}_2\text{O}_3 \cdot 2\text{SiO}_2 \cdot 9/2\text{H}_2\text{O}$. The influence of NaOH/CFA mass ratio on the product was analyzed using CFA-based molecular sieves with a calcination temperature of 750 °C, a hydrothermal time of 6 h, and a solid-to-liquid ratio of 1:6. Combined with Fig. 2A, it can be observed that the NaOH/CFA mass ratio has a significant impact on the product. When the NaOH/CFA mass ratio is 1.2, the Zeolite A (PDF 39-0222) in the synthesized molecular sieve gradually becomes more complete, with increasing peak intensity. However, as the NaOH/CFA mass ratio continues to increase, the presence of impurity peaks near the characteristic peaks also increases. This may be attributed to excessive alkali sources activating and dissolving more inert silicon and aluminum, leading to the formation of other impurity crystals. This could be attributed to excessive activation of alkaline sources, resulting in the dissolution of more inert silicon and aluminum, leading to the formation of other impurity crystals. In Fig. 3A and C, the SEM images show a well-defined and regular three-dimensional structure with fewer irregular substances. However, with a higher alkali ash ratio, as shown in Fig. 2A (D3 and D4), the three-dimensional structure exhibits more fragmented and irregular substances, and some structures are damaged, with a small portion of the calcination product forming aggregates. Figure 2C and D demonstrate the influence of the alkali ash ratio on particle size uniformity, with a NaOH/CFA mass ratio of 1.2 showing better particle size uniformity compared to 1.4. At this point, the specific surface area is 24.928 m^2/g . When the mass ratio is 1, 1.4, and 1.6, the specific surface areas are 12.130 m^2/g , 69.432 m^2/g , and 97.345 m^2/g respectively. More details

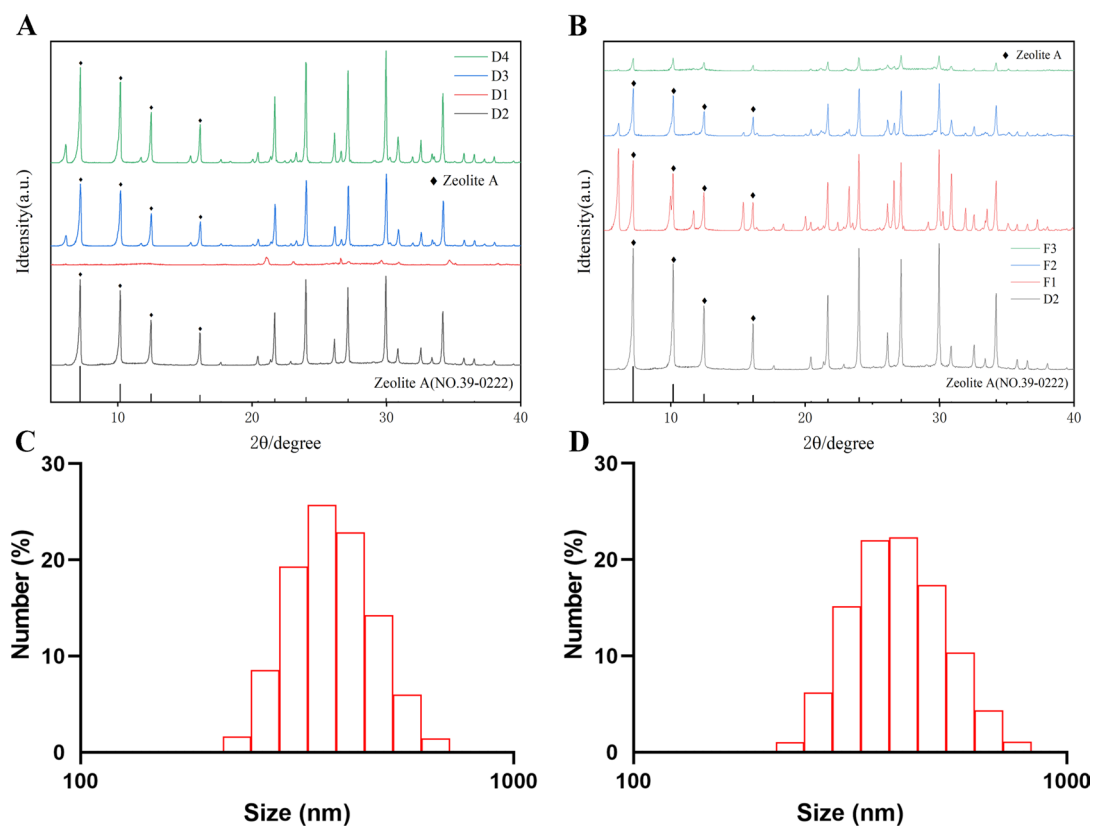


Fig. 2. Characterization of Zeolite A. (A) XRD image of (D1 ~ D4) (NaOH/CFA = 1, 1.2, 1.4, 1.6 respectively, Solid/liquid = 1:6). (B) XRD image of (F1 ~ F4) (NaOH/CFA = 1.2, 750 °C). (C) Hydrodynamic size distribution of D2 (NaOH/CFA = 1.2, Solid/liquid = 1:6, 750 °C). (D) Hydrodynamic size distribution of D1 (NaOH/CFA = 1.4, Solid/liquid = 1:6, 750 °C).

about the SEM, XRD, and particle size distribution of sample D1 ~ D4 are provided in Figs. S1–S3 supplementary information. Considering the zeolite purity, particle size uniformity, crystallinity, and cost, a NaOH/CFA mass ratio of 1.2 is deemed more suitable.

Calcination temperature

The mixture of fly ash and alkali melts at high temperature 700 °C, causing the crystalline phase to transform into zeolite products, which are rich in sodium salts of silicon and aluminum. Comparing the SEM images in Fig. 3A D2 and B E1, at lower calcination temperatures, the edges are not significant and the shape is irregular. Some samples fail to form a cubic morphology. However, as the calcination temperature increases, the edges become more prominent and the shape becomes more regular. Under the same treatment conditions, when the calcination temperature is lower (650 °C), it is more difficult to form regular-shaped A-type zeolites in the product. The surface of the product appears rough, mostly consisting of irregularly shaped, unevenly sized particles, with a specific surface area of 35.699 m²/g. As the temperature increases (700 °C), the cubic morphology gradually becomes apparent, edges start to form, and irregular particles decrease, though they still dominate the field of view, with a specific surface area of 45.976 m²/g at this point. When the temperature reaches 750 °C, irregular particles are less visible in the field of view, mostly replaced by well-defined cubic shapes, with more uniform particle sizes and increased regularity, resulting in a specific surface area of 24.928 m²/g, the lowest value obtained. With further increase in the calcination temperature (800 °C), due to excessively high temperature, the cubic structure of particles is disrupted, reverting to irregularly shaped, unevenly sized particles, with a specific surface area of 46.127 m²/g. At the same time, the irregularities attached to the cubes gradually decrease. Therefore, we believe that the appropriate calcination temperature is crucial for the growth and formation of the zeolite crystal phase. In addition, the TEM of sample D2 is shown in Fig. 3E, and it shows good purity and uniformity of the crystal structures. Considering the relationship between the zeolite structure and energy consumption, a calcination temperature of 750 °C is considered more suitable.

Solid–liquid ratio

Analyzed under the most favorable conditions among other parameters, the effect of the solid–liquid ratio on the growth and crystal phase of zeolite was analyzed when the NaOH/CFA ratio was 1.2, the calcination temperature was 750 °C, and the hydrothermal time was 6 h. As shown in Fig. 3A D2 and D F1, when the solid–liquid ratio increased to 1:6, the amorphous SiO₂ and Al₂O₃ in the solution were fully dissolved. At this point, the purity of the Zeolite A molecular sieve reached its maximum, and the SEM image mainly showed a clear cubic

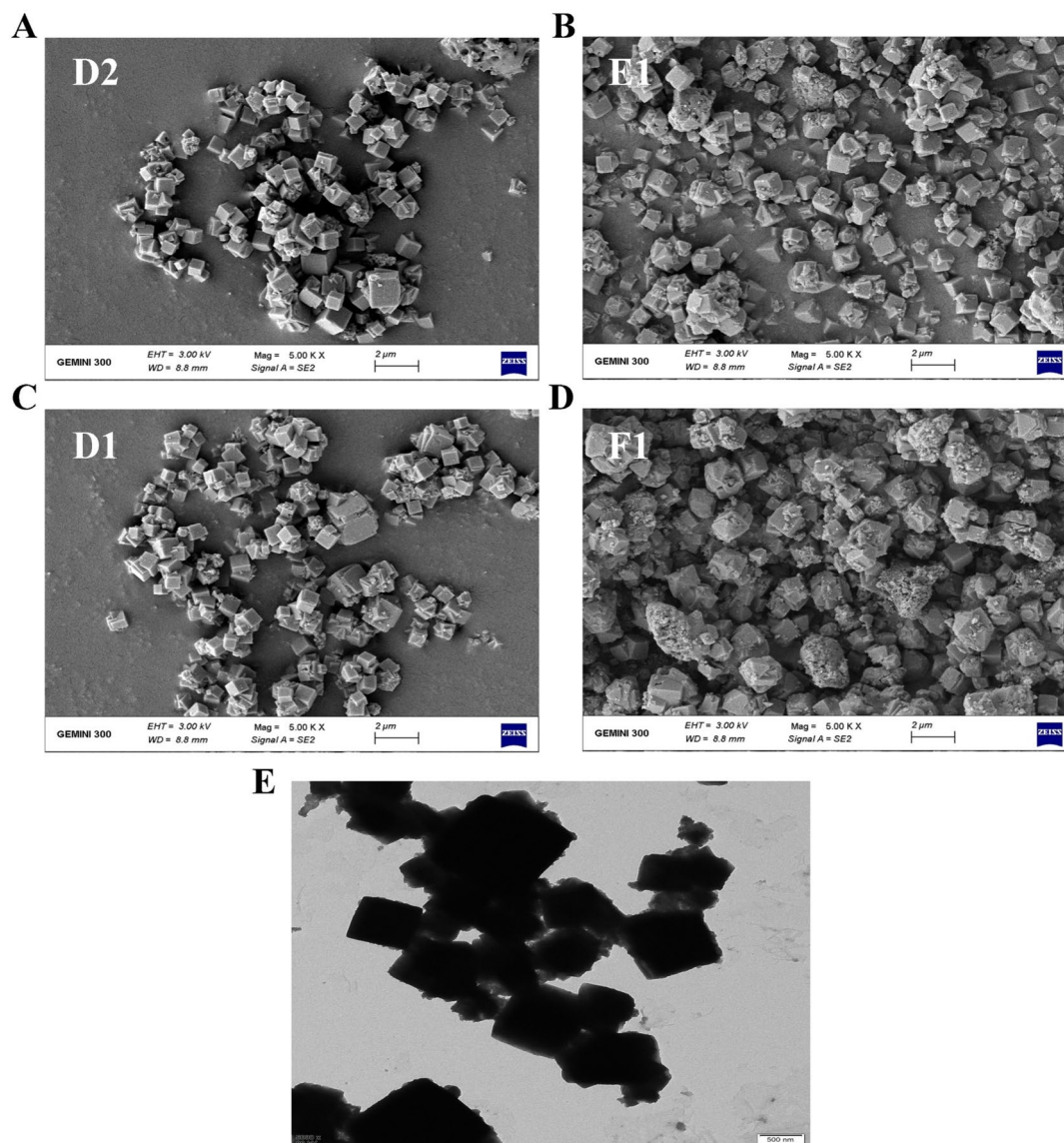


Fig. 3. Characterization of Zeolite A. (A) SEM image of D2 (NaOH/CFA = 1.2, Solid/liquid = 1:6, 750 °C) (scale bar = 2 μm). (B) SEM image of E1 (NaOH/CFA = 1.2, Solid/liquid = 1:6, 650 °C) (scale bar = 2 μm). (C) SEM image of D1 (NaOH/CFA = 1.0, Solid/liquid = 1:6, 750 °C) (scale bar = 2 μm). (D) SEM image of F1 (NaOH/CFA = 1.2, Solid/liquid = 1:5, 750 °C) (scale bar = 2 μm). (E) TEM image of D2 (NaOH/CFA = 1.2, Solid/liquid = 1:6, 750 °C) (scale bar = 500 nm).

structure with distinct edges. There were also fewer other granular substances, and the crystallization rate of the product was relatively high. When the solid–liquid ratio exceeded 1:6, the characteristic peaks of the Zeolite A continuously decreased with the increase of the liquid, indicating a decrease in crystal content and a decrease in crystallinity, as shown in Fig. 2B. We hypothesize that this phenomenon may be attributed to the reduction in the concentrations of silicon and aluminum in the system as the solid-to-liquid ratio exceeds 1:6. This reduction leads to a lower concentration of the aluminosilicate gel, which hinders the interaction and assembly of gel particles, consequently affecting the growth of the molecular sieve nuclei. Additionally, an insufficient amount of water can result in excessively high alkalinity, which may lead to the formation of undesired crystalline phases. Therefore, a solid–liquid ratio of 1:6 is considered more appropriate.

Adsorption performance of ammonia–nitrogen

Toxicity of ammonia–nitrogen analysis to hemoglobin of human

In water, nitrifying bacteria convert ammonia into nitrite and nitrate³. Nitrate in drinking water can completely absorbed into the blood, where a portion is converted to nitrite³⁰. Nitrite then reacts with blood to produce methemoglobin (MetHb). The Pathways for the formation of MetHb: 1. Nitrite (NO_2^-) oxidizes hemoglobin (Hb), leading to the production of nitrogen oxide (NO) and MetHb. 2. NO can then react with oxyhemoglobin (HbO_2) to form MetHb and NO_3^- . 3. Nitrite reacting with HbO_2 can also generate MetHb and NO_3^- ³¹. The 3D

structure of HbO₂ and MetHb are shown in Fig. 4A and B, respectively. The Fe(III) in MetHb loses the capacity to carry O₂. Therefore, it is crucial to find proper conditions to remove ammonia–nitrogen in water.

Adsorption capacity and removal rate of ammonia–nitrogen

The effect of adsorption time. Under the conditions of adding 0.05 L of 100 mg/L ammonia nitrogen solution and 0.05 g of CFA molecular sieve, according to Fig. 5B, the adsorption capacity and removal efficiency of ammonia nitrogen increase with the increase of adsorption time. Within 30 min, the adsorption rate is fast, and the removal rate rapidly increases to 24.05%, with an adsorption capacity of 24.05 mg·g⁻¹. This is because at the beginning of adsorption, the concentration of ammonia–nitrogen in the solution is still relatively high, while the concentration of ammonia–nitrogen on the surface of the zeolite is low, resulting in a significant concentration difference between the two. Since there are many available adsorption sites at the beginning of adsorption, the adsorption rate is fast, leading to a significant increase in adsorption capacity. As the adsorption time continues to increase, both the removal rate and adsorption capacity continue to increase, but the rate of increase slows down. At 70 min, the removal rate reaches 32.56% and the adsorption capacity is 32.56 mg·g⁻¹. As the concentration of ammonia–nitrogen in the solution gradually decreases, the concentration of ammonia–nitrogen on the surface of the zeolite becomes higher, resulting in a smaller concentration difference between the two. As a result, the available adsorption sites gradually decrease and the adsorption capacity increases slowly.

The effect of initial concentration. Under the conditions of adding 50 ml of 60 mg/L, 80 mg/L, 100 mg/L, 150 mg/L, and 200 mg/L ammonia nitrogen solutions separately, with 0.05 g of CFA molecular sieve. With the increase in the initial concentration of the ammonia–nitrogen solution, the adsorption capacity of CFA-based zeolite for ammonia–nitrogen shows a gradual increase trend. This may be due to the presence of more adsorbates available for ion exchange and adsorption in high-concentration ammonia–nitrogen solutions. Additionally, the large concentration difference between the high-concentration solution and the zeolite surface facilitates the entry of adsorbates into the interior of the zeolite, thereby increasing the adsorption capacity.

However, after reaching a certain adsorption capacity, the adsorption capacity of zeolite for ammonia–nitrogen gradually weakens as the concentration of the ammonia–nitrogen solution continues to increase. This is because, under a fixed amount of zeolite, its maximum adsorption capacity is limited. In Fig. 5A, at a concentration of 100 mg/L, the adsorption capacity is 32.90 mg/g, with a removal rate of 32.90%. As the concentration increases, although the adsorption capacity increases, the removal rate gradually decreases, indicating a poorer removal effect. This means that as the concentration continues to increase, although it can promote the penetration of adsorbates into deeper parts of the zeolite framework, thereby increasing the adsorption capacity, the magnitude of this increase gradually diminishes.

The effect of temperature. Under the conditions of adding 0.05 L of 100 mg/L ammonia nitrogen solution and 0.05 g of CFA zeolite at 25 °C, 30 °C, 35 °C, 40 °C, and 45 °C, according to Fig. 5C, the effect of temperature on the adsorption of ammonia–nitrogen by zeolite shows an initial decrease followed by an increase, with an overall decreasing trend. At a temperature of 25 °C, the removal rate is 32.80%, and the adsorption capacity is 32.80 mg/g. The lowest adsorption capacity is observed at 45 °C, with a value of 21.71 mg/g and a removal rate of 21.71%. The decrease in removal rate and adsorption capacity from 25 °C to 30 °C may be attributed to the effect of temperature on van der Waals forces, weakening these forces. However, from 30 °C to 40 °C, both the removal rate and adsorption capacity increase. This could be due to the initially high pH value of the solution, leading to the hydrolysis reaction of ammonium ions during heating, resulting in a decrease in pH reaching the optimal range. Consequently, there is a temporary increase in adsorption capacity, affecting the adsorption onto the zeolite, and this factor has a greater impact than the changes in van der Waals forces, thereby increasing the zeolite's adsorption capacity for ammonia nitrogen. As the temperature continues to rise, van der Waals forces continue to weaken, and pH becomes too low, causing a rapid decrease in both removal rate and adsorption capacity.

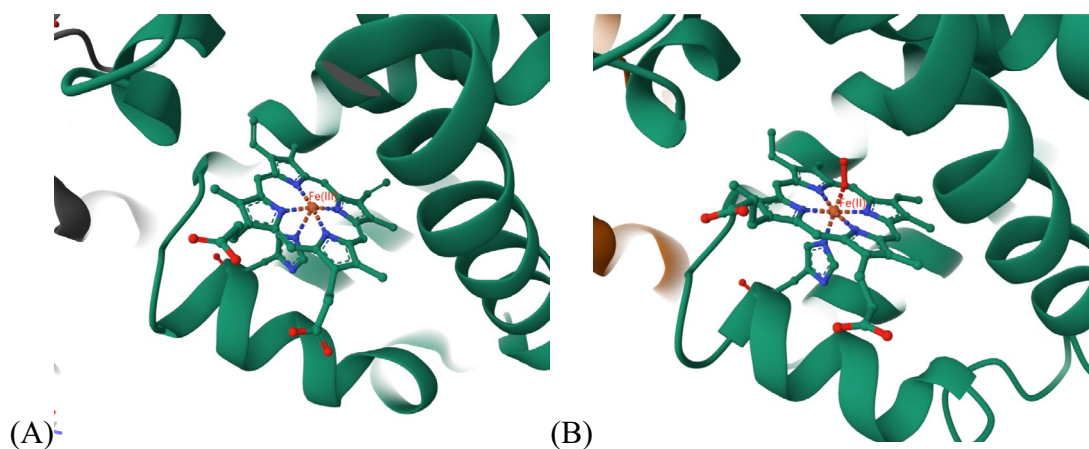


Fig. 4. Three-dimensional representation of (A) MetHb (PDBID: 1JY7) and (B) HbO₂ (PDBID: 1HHO). The Fe(III) in MetHb is unable to bind O₂, whereas the Fe(II) in Hb is capable of binding O₂.

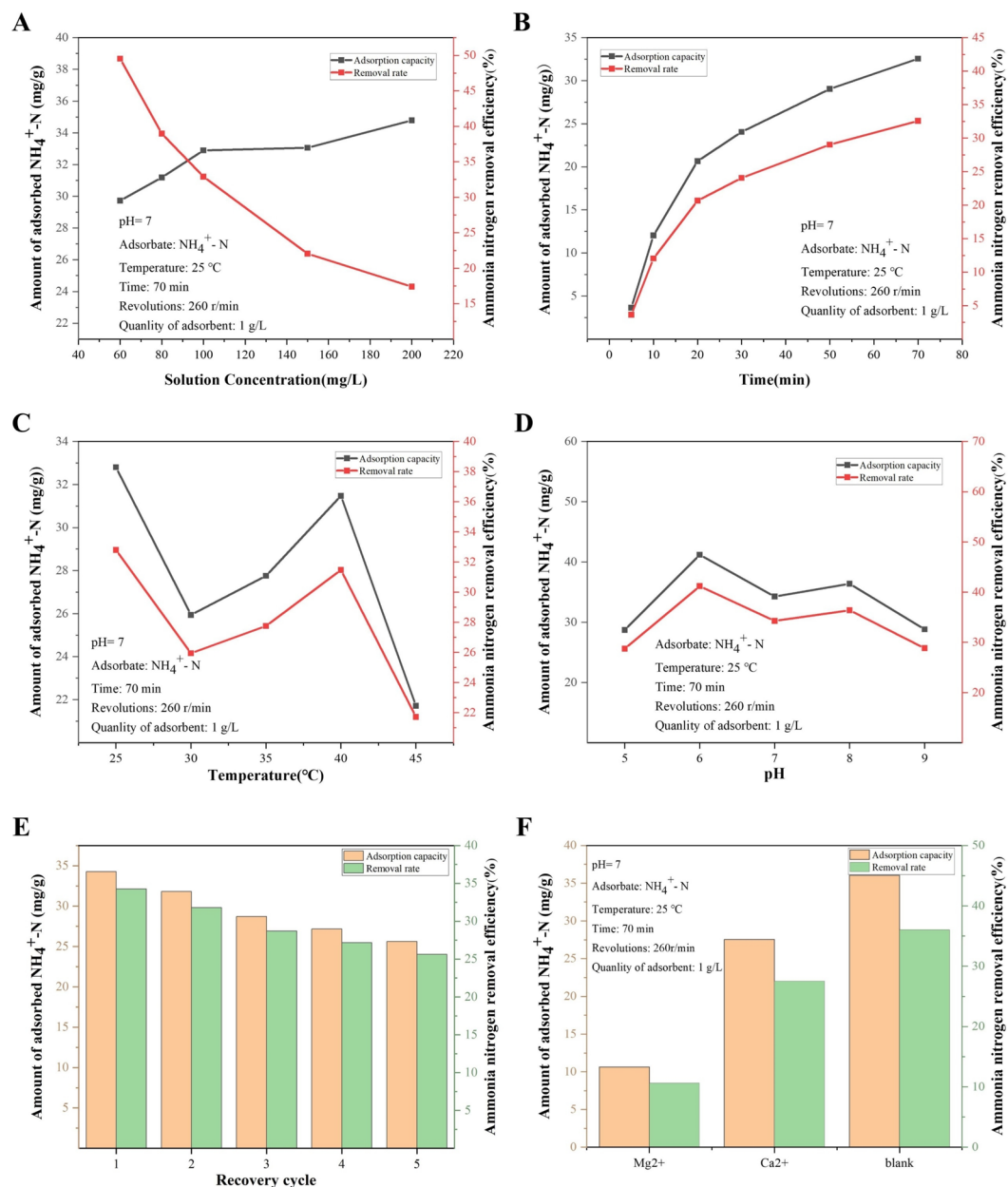


Fig. 5. Ammonia–nitrogen adsorption of zeolite A. (A) Effect of adsorbent dosage on adsorption. (B) Effect of adsorption time on adsorption. (C) Effect of adsorption temperature on adsorption. (D) Effect of adsorption pH on adsorption. (E) Effect of regeneration times of zeolite molecular sieve on ammonia nitrogen adsorption (F) Effect of competitive cations on adsorption.

The effect of pH. Under the conditions of adding 0.05 L of 100 mg/L ammonia nitrogen solution and 0.05 g of CFA zeolite at pH 5, 6, 7, 8, and 9, the results are shown in Fig. 5D. The removal efficiency of ammonia–nitrogen is highest between pH 6 and 8, and the adsorption capacity of ammonia–nitrogen is higher within the pH range of 6 to 8, with a gradual change. The removal efficiency reaches 41.20%, and the adsorption capacity reaches 41.20 mg/g. Outside of this range, both the removal efficiency and adsorption capacity of ammonia–nitrogen are lower. When the pH value of the solution is low, it means that there is a higher concentration of H⁺ in the solution. In this case, ammonia–nitrogen mainly exists in the form of NH₄⁺. Due to the smaller ionic radius of H⁺ compared to NH₄⁺, H⁺ is more likely to enter the internal pores of the zeolite. This means that the internal pores of the zeolite are occupied by H⁺, reducing its adsorption capacity for NH₄⁺ and resulting in poor adsorption performance for ammonia–nitrogen. In the other side, the hydrated shell surrounding the ions works as a barrier to the adsorption on the adsorbent surface, which resulting in poor adsorption performance as well. Conversely, when the pH value of the solution is high, it means that there is a higher concentration of OH⁻ in the solution. In this case, ammonia–nitrogen mainly exists in the form of hydrated ammonia molecules. Due to the presence of OH⁻, the ion exchange interaction between the zeolite and NH₄⁺ is weakened. Therefore, the zeolite mainly

adsorbs hydrated ammonia molecules rather than NH_4^+ , resulting in overall poor adsorption performance for ammonia–nitrogen.

The effect of competitive cations. At 25 °C, with an ammonia–nitrogen concentration of 100 mg/L and a solution pH of 7, when the dosage of CFA zeolite is 1 g/L, Fig. 5F shows that without competitive cations, after 70 min of adsorption, the adsorption capacity and removal efficiency of ammonia–nitrogen by the zeolite are 36.04 mg/g and 36.04%, respectively. However, when an equal concentration of magnesium ions is added, the adsorption capacity and removal efficiency decrease to 10.62 mg/g and 10.62%, respectively. When an equal concentration of calcium ions is used, the adsorption capacity and removal efficiency of ammonia–nitrogen decrease by 27.54 mg/g and 27.54%, respectively. It can be seen that both metal ions compete with the zeolite for the adsorption of ammonia–nitrogen, and the influence of Mg^{2+} is significantly greater than that of Ca^{2+} . Under other similar and appropriate conditions, the hydration energy and ionic radius of metal ions are important factors affecting the adsorption capacity of zeolite for metal ions³². According to the hydration entropy values of metal ions obtained from the hydration entropy table, the hydration entropy value of Mg^{2+} is greater than that of Ca^{2+} , indicating that the influence of Mg^{2+} is greater than that of Ca^{2+} .

Based on above discussion, the adsorption mechanism of ammonia–nitrogen using CFA zeolite primarily involves ion exchange, where NH_4^+ are exchanged with cations in the zeolite. This process is influenced by contact time, initial concentration, temperature, and pH. Initially rapid, the adsorption rate slows as sites become occupied. Higher initial concentrations increase adsorption until saturation. Temperature impacts efficiency, with optimal adsorption at a pH of 6 to 8. Low pH leads to competition between H^+ and NH_4^+ ions, while high pH converts NH_4^+ to less effectively adsorbed NH_3 . Collectively, these mechanisms contribute to the effective adsorption of ammonia–nitrogen by CFA zeolite, making it a promising material for removing ammonia from aqueous solutions.

In this section, we found that the highest the adsorption capacity reaches 41.20 mg/g at 25 °C, solution pH = 6, and the dosage of CFA zeolite is 1 g/L. Compare to previous published work^{33–38} (The details of comparison is shown in Table S1 of supplementary information), the molecular sieve prepared in this work shown the highest adsorption capacity, and show promising potential for wastewater treatment applications.

Regeneration of zeolite A molecular sieve

Regeneration technology for adsorbents is of great significance in the fields of environmental protection and resource recycling. It not only reduces the cost of adsorbent usage but also minimizes the issues of handling and disposal of waste adsorbents. In practical applications, the regenerability of adsorbents is an important indicator for evaluating their economic and environmental performance. It should note here, based on the previous work^{39,40}, we conducted 10 regeneration cycles to assess the regenerability of the adsorbents. The adsorption amounts and removal rates for cycles 1–5 are presented in Fig. 5E, while the data for all 10 cycles can be found in Fig. S4 of the supplementary information. It can be concluded that the adsorption amounts for the first two cycles are 34.28 and 31.81, with removal rates of 34.28% and 31.81% respectively. In the fifth cycle removal rates of 25.6% as show in the Fig. 5E. In the 10th cycle removal rates of 23.7%. As the number of regeneration cycles for the zeolite molecular sieve increases, its ammonia nitrogen adsorption efficiency gradually decreases and eventually stabilizes. (As shown in Fig. S4) Therefore, this zeolite exhibits good regenerability, with a slight decrease in the adsorption amount but still at a satisfactory adsorption level. The decrease may be due to some adsorbates in the initial adsorption entering the deeper and smaller crystal pores, making them difficult to remove.

Zeolite molecular sieve adsorption kinetics and isotherms analysis

In the study of the adsorption behavior of ammonia–nitrogen on CFA-based Zeolite A, we used the pseudo-first-order and pseudo-second-order kinetic models for simulation and analysis, as shown in Fig. 6A. The simulation results showed that the pseudo-second-order kinetic model had a significantly higher coefficient of determination ($R^2 = 99.71\%$) compared to the pseudo-first-order kinetic model ($R^2 = 97.764\%$). Therefore, the pseudo-second-order kinetic model proves to be more effective in elucidating the kinetics of ammonia–nitrogen adsorption on NaA zeolite molecular sieve. This finding suggests that the adsorption of ammonia–nitrogen on zeolite is predominantly governed by chemisorption rather than physisorption, consistent with previous research⁴. To enhance the performance of adsorbents in future studies or industrial applications, the following strategies can be applied: 1. *Surface modification*: Enhance the number of active sites on the adsorbent through surface modification or functionalization. This will enhance the interaction between the adsorbent and the target substance, ultimately improving adsorption efficiency and selectivity. 2. *Optimization of pore structure*: Control the pore structure of the adsorbent, including pore size, volume, and distribution. This will increase the adsorption surface area and improve diffusion rate, ultimately enhancing adsorption efficiency.

The overall adsorption rate and capacity can be controlled by one or multiple steps in adsorption process. Adsorption mechanism of ammonia–nitrogen on CFA-based Zeolite A was further studied by the intraparticle diffusion model. The analysis of the experimental data in Fig. 6B shows that the fitted data of the adsorption capacity q_t and the time $t^{0.5}$ can be divided into two linearly related stages, exhibiting different trends in adsorption rate and diffusion resistance. In the first stage, the adsorption rate K_1 is larger and the diffusion boundary layer thickness C_1 is smaller. In the second stage, the adsorption rate K_2 decreases, while the diffusion boundary layer thickness C_2 increases. This suggests that as the adsorption progresses, the internal diffusion resistance of the particles gradually increases, leading to a decrease in adsorption rate and eventually reaching equilibrium, where both parameters stabilize. Therefore, the first stage has a significant impact on both the adsorption rate and capacity.

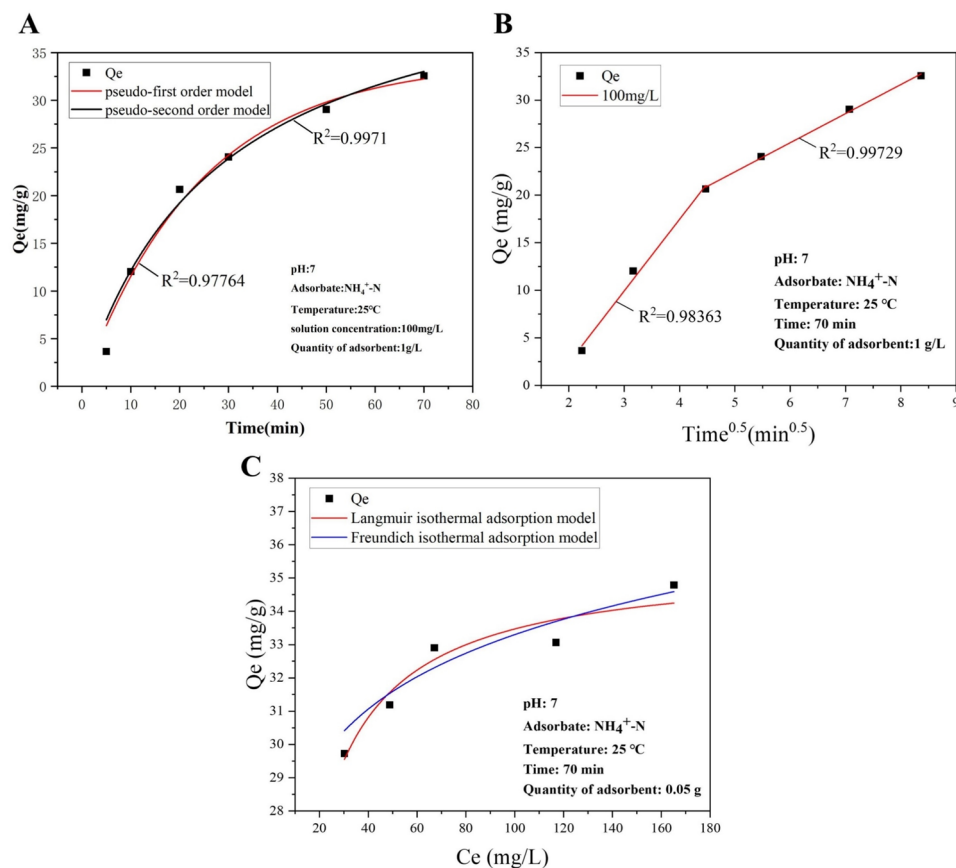


Fig. 6. Adsorption curve model of zeolite A. (A) Fitting curves of pseudo-first-order kinetic model. (B) Fitting curves of quasi-internal diffusion model. (C) Fitting curves of pseudo-isothermal adsorption model.

Adsorption isotherm can reflect the adsorption performance of adsorbents and the equilibrium distribution of adsorbates in the liquid–solid phases. Through static adsorption experiments, the effective adsorption capacity during continuous dynamic adsorption can be estimated, providing parameter basis for the selection of processes and equipment for treating ammonia–nitrogen-containing wastewater. Langmuir isotherm model and Freundlich isotherm model are two commonly used isotherm models. As shown in Fig. 6C, the Langmuir model can better fit the experimental data, indicating that the adsorption process of ammonia–nitrogen on Zeolite A conforms to the assumptions of the Langmuir model. This suggests that the adsorption mechanism primarily involves uniform monolayer adsorption on the surface without intermolecular interactions.

Conclusions

In this research, a zeolite A molecular sieve was synthesized from CFA for wastewater treatment, exhibiting exceptional adsorption capabilities. The hierarchical microporous structure of the zeolite provided a high surface area and rapid mass transfer, enhancing ammonia–nitrogen adsorption. The adsorption process was pH adaptable, maintaining maximum capacity within the standard pH range (6–8) and was robust against competing cations. Kinetically, the adsorption followed a pseudo-second-order model, indicating that the adsorption of ammonia–nitrogen on zeolite is primarily controlled by chemisorption rather than physisorption. The adsorption process can be divided into two stages: an initial rapid phase with a smaller diffusion boundary layer, followed by a slower phase with increased resistance as equilibrium approached. The adsorption isotherms of ammonia–nitrogen on zeolite A conformed to the assumptions of the Langmuir model, suggesting that the adsorption mechanism primarily involves uniform monolayer adsorption on the surface without intermolecular interactions.

Overall, the CFA-based zeolite A molecular sieve demonstrated high adsorption capacity, quick adsorption kinetics, and reusability, making it a promising adsorbent for sustainable wastewater treatment. Its application not only utilizes waste materials efficiently but also aligns with principles of environmental sustainability, offering a valuable solution for ammonia–nitrogen removal in wastewater treatment processes.

Data availability

All data generated or analyzed during this study available from the corresponding author on reasonable request.

Received: 30 March 2024; Accepted: 3 September 2024

Published online: 10 September 2024

References

- Lyu, S. D., Chen, W. P., Zhang, W. L., Fan, Y. P. & Jiao, W. T. Wastewater reclamation and reuse in China: Opportunities and challenges. *J. Environ. Sci.* **39**, 86–96. <https://doi.org/10.1016/j.jes.2015.11.012> (2016).
- Wang, P., Sun, Q., Zhang, Y. J. & Cao, J. Alkali-dissolving hydrothermal synthesis of zeolite P from fly ash. *Micro Nano Lett.* **14**, 572–576. <https://doi.org/10.1049/mnl.2018.5650> (2019).
- Qin, W. *et al.* Ammonia-oxidizing bacteria and archaea exhibit differential nitrogen source preferences. *Nat. Microbiol.* <https://doi.org/10.1038/s41564-023-01593-7> (2024).
- Comly, H. H. Cyanosis in infants caused by nitrates in well water. *J. Am. Med. Assoc.* **129**, 112–116. <https://doi.org/10.1001/jama.1945.02860360014004> (1945).
- Dong, Y., Yuan, H., Zhang, R. & Zhu, N. Removal of ammonia nitrogen from wastewater: A review. *Trans. Asabe* **62**, 1767–1778. <https://doi.org/10.13031/trans.13671> (2019).
- Wang, M. Q., Xu, D. F., Ma, H., Li, B. & Howard, A. Synthesis of NaA zeolite from foundry dust and its adsorption capacity of ammonia. *J. Environ. Manag.* **331**, 117297. <https://doi.org/10.1016/j.jenvman.2023.117297> (2023).
- Lyu, S., Chen, W., Zhang, W., Fan, Y. & Jiao, W. Wastewater reclamation and reuse in China: Opportunities and challenges. *J. Environ. Sci.* **39**, 86–96 (2016).
- Wang, Y. F., Lin, F. & Pang, W. Q. Ammonium exchange in aqueous solution using Chinese natural clinoptilolite and modified zeolite. *J. Hazard. Mater.* **142**, 160–164. <https://doi.org/10.1016/j.jhazmat.2006.07.074> (2007).
- Park, J., Choe, J. K., Lee, W. & Bae, S. Highly fast and selective removal of nitrate in groundwater by bimetallic catalysts supported by fly ash-derived zeolite Na-X. *Environ. Sci.-Nano* **7**, 3360–3371. <https://doi.org/10.1039/d0en00721h> (2020).
- Al-Jubouri, S. M., Al-Batty, S. I. & Holmes, S. M. Using the ash of common water reeds as a silica source for producing high purity ZSM-5 zeolite microspheres. *Microporous Mesoporous Mater.* **316**, 110953. <https://doi.org/10.1016/j.micromeso.2021.110953> (2021).
- Jalali, S., Arjmand, M., Ramavandi, B. & Nosratinia, F. Elimination of amoxicillin using zeolite Y-sea salt as a good catalyst for activation of hydrogen peroxide: Investigating degradation pathway and the effect of wastewater chemistry. *J. Environ. Manag.* **302**, 114045. <https://doi.org/10.1016/j.jenvman.2021.114045> (2022).
- Ayati, A. *et al.* Insight into the adsorptive removal of ibuprofen using porous carbonaceous materials: A review. *Chemosphere* **323**, 138241. <https://doi.org/10.1016/j.chemosphere.2023.138241> (2023).
- Ahmadpour, A. *et al.* Dual-purpose magnetic κ -carrageenan/montmorillonite hydrogel for carrying and removal of tetracycline from aqueous medium. *Inorg. Chem. Commun.* **156**, 111274. <https://doi.org/10.1016/j.inoche.2023.111274> (2023).
- Al-Jubouri, S. M. *et al.* Silver oxide-zeolite for removal of an emerging contaminant by simultaneous adsorption-photocatalytic degradation under simulated sunlight irradiation. *J. Photochem. Photobiol. A Chem.* **442**, 114763. <https://doi.org/10.1016/j.jphotochem.2023.114763> (2023).
- Musyoka, N. M., Petrik, L. F., Fatoba, O. O. & Hums, E. Synthesis of zeolites from coal fly ash using mine waters. *Miner. Eng.* **53**, 9–15. <https://doi.org/10.1016/j.mineng.2013.06.019> (2013).
- Cardoso, A. M., Horn, M. B., Ferret, L. S., Azevedo, C. M. N. & Pires, M. Integrated synthesis of zeolites 4A and Na-P1 using coal fly ash for application in the formulation of detergents and swine wastewater treatment. *J. Hazard. Mater.* **287**, 69–77. <https://doi.org/10.1016/j.jhazmat.2015.01.042> (2015).
- Basaldella, E. I., Bonetto, R. & Tara, J. C. Synthesis of NaY zeolite on preformed kaolinite spheres. Evolution of zeolite content and textural properties with the reaction time. *Ind. Eng. Chem. Res.* **32**, 751–752 (1993).
- Amei, A. E., Fatoba, O. O., Musyoka, N. M., Louis, B. & Petrik, L. F. Transformation of fly ash based nanosilica extract to BEA zeolite and its durability in hot liquid. *Microporous Mesoporous Mater.* **305**, 110332. <https://doi.org/10.1016/j.micromeso.2020.110332> (2020).
- Yang, K., Zhang, X., Chao, C., Zhang, B. & Liu, J. In-situ preparation of NaA zeolite/chitosan porous hybrid beads for removal of ammonium from aqueous solution. *Carbohydr. Polym.* **107**, 103–109. <https://doi.org/10.1016/j.carbpol.2014.02.001> (2014).
- Safie, N. N., Yaser, A. & Hilal, N. Ammonium ion removal using activated zeolite and chitosan. *Asia-Pac. J. Chem. Eng.* <https://doi.org/10.1002/apj.2448> (2020).
- Chang, M. Y. & Juang, R. S. Adsorption of tannic acid, humic acid, and dyes from water using the composite of chitosan and activated clay. *J. Colloid Interface Sci.* **278**, 18–25. <https://doi.org/10.1016/j.jcis.2004.05.029> (2004).
- Domínguez-Vargas, J. R., Gonzalez, T., Palo, P. & Cuerda-Corrae, E. M. Removal of carbamazepine, naproxen, and trimethoprim from water by amberlite XAD-7: A kinetic study. *Clean Soil Air Water* **41**, 1052–1061. <https://doi.org/10.1002/clean.201200245> (2013).
- Üner, O., Geçgel, Ü. & Bayrak, Y. Adsorption of methylene blue by an efficient activated carbon prepared from *Citrullus lanatus* Rind: Kinetic, isotherm, thermodynamic, and mechanism analysis. *Water Air Soil Pollut.* <https://doi.org/10.1007/s11270-016-2949-1> (2016).
- Luo, J. *et al.* Experimental and modeling study of methane adsorption on activated carbon derived from anthracite. *J. Chem. Eng. Data* **56**, 4919–4926. <https://doi.org/10.1021/je200834p> (2011).
- Faria, P. C., Orfao, J. J. & Pereira, M. F. Adsorption of anionic and cationic dyes on activated carbons with different surface chemistries. *Water Res.* **38**, 2043–2052. <https://doi.org/10.1016/j.watres.2004.01.034> (2004).
- Al-Jubouri, S. M., Al-Jendeel, H. A., Rashid, S. A. & Al-Batty, S. Green synthesis of porous carbon cross-linked Y zeolite nanocrystals material and its performance for adsorptive removal of a methyl violet dye from water. *Microporous Mesoporous Mater.* **356**, 112587. <https://doi.org/10.1016/j.micromeso.2023.112587> (2023).
- Ibrahim, N. H. & Al-Jubouri, S. M. Facile preparation of dual functions zeolite-carbon composite for zinc ion removal from aqueous solutions. *Asia-Pac. J. Chem. Eng.* **19**, e2967. <https://doi.org/10.1002/apj.2967> (2024).
- Xie, W. M. *et al.* Accelerated crystallization of magnetic 4A-zeolite synthesized from red mud for application in removal of mixed heavy metal ions. *J. Hazard. Mater.* **358**, 441–449. <https://doi.org/10.1016/j.jhazmat.2018.07.007> (2018).
- Al-Jubouri, S. M., Al-Batty, S. I., Ramsden, R., Tay, J. & Holmes, S. M. Elucidation of the removal of trivalent and divalent heavy metal ions from aqueous solutions using hybrid-porous composite ion-exchangers by nonlinear regression. *Desalin. Water Treat.* **236**, 171–181. <https://doi.org/10.5004/dwt.2021.27707> (2021).
- Rosenfield, A. B. & Huston, R. Infant methemoglobinemia in Minnesota due to nitrates in well water. *Minn. Med.* **33**, 789–796 (1950).
- Cavaiuolo, M. & Ferrante, A. Nitrates and glucosinolates as strong determinants of the nutritional quality in rocket leafy salads. *Nutrients* **6**, 1519–1538 (2014).
- Bo, Y. *Study on Removal of Cd²⁺ in Aqueous Solution on Zeolite 4A* (Shenyang Agricultural University, 2011).
- Xue, R. *et al.* Simultaneous removal of ammonia and N-nitrosamine precursors from high ammonia water by zeolite and powdered activated carbon. *J. Environ. Sci.* **64**, 82–91. <https://doi.org/10.1016/j.jes.2017.02.010> (2018).
- Muscarella, S. M., Badalucco, L., Cano, B., Laudicina, V. A. & Mannina, G. Ammonium adsorption, desorption and recovery by acid and alkaline treated zeolite. *Bioresour. Technol.* **341**, 125812. <https://doi.org/10.1016/j.biortech.2021.125812> (2021).

35. Wasielewski, S., Rott, E., Minke, R. & Steinmetz, H. Evaluation of different clinoptilolite zeolites as adsorbent for ammonium removal from highly concentrated synthetic wastewater. *Water* **10**, 584 (2018).
36. Wang, M. *et al.* A novel mesoporous zeolite-activated carbon composite as an effective adsorbent for removal of ammonia-nitrogen and methylene blue from aqueous solution. *Bioresour. Technol.* **268**, 726–732. <https://doi.org/10.1016/j.biortech.2018.08.037> (2018).
37. Xu, Q. *et al.* Simultaneous removal of ammonia and phosphate using green synthesized iron oxide nanoparticles dispersed onto zeolite. *Sci. Total Environ.* **703**, 135002 (2020).
38. Lu, Q. *et al.* A novel approach of using zeolite for ammonium toxicity mitigation and value-added Spirulina cultivation in wastewater. *Bioresour. Technol.* **280**, 127–135 (2019).
39. Huang, Z. *et al.* Synthesis of 4A zeolite molecular sieves by modifying fly ash with water treatment residue to remove ammonia nitrogen from water. *Sustainability* **16**, 5683 (2024).
40. de Oliveira, L. H. *et al.* Influence of regeneration conditions on cyclic CO₂ adsorption on NaA zeolite at high pressures. *J. CO₂ Util.* **67**, 102296. <https://doi.org/10.1016/j.jcou.2022.102296> (2023).

Acknowledgements

This work was supported by the Natural Science Foundation of Zhejiang Province (No. LQ21H300008), Scientific Research Fund of Zhejiang Provincial Education Department (No. Y202352312) and Zhejiang Health Information Association Research Program (No. 2023XHSZ-Z05).

Author contributions

Q.J., J.H., Y.W., B.C., and K.T. are responsible for performing experiments, synthesizing materials, characterizing samples, conducting formal analysis, and preparing the initial draft of the manuscript. K.Y., H.W., and X.X. are involved in conceptualization, research planning and management, supervising the research project, conducting detailed analysis and discussion, and revising the manuscript.

Competing interests

The authors declare no competing interests.

Additional information

Supplementary Information The online version contains supplementary material available at <https://doi.org/10.1038/s41598-024-72067-x>.

Correspondence and requests for materials should be addressed to K.Y., H.W. or X.X.

Reprints and permissions information is available at www.nature.com/reprints.

Publisher's note Springer Nature remains neutral with regard to jurisdictional claims in published maps and institutional affiliations.

Open Access This article is licensed under a Creative Commons Attribution-NonCommercial-NoDerivatives 4.0 International License, which permits any non-commercial use, sharing, distribution and reproduction in any medium or format, as long as you give appropriate credit to the original author(s) and the source, provide a link to the Creative Commons licence, and indicate if you modified the licensed material. You do not have permission under this licence to share adapted material derived from this article or parts of it. The images or other third party material in this article are included in the article's Creative Commons licence, unless indicated otherwise in a credit line to the material. If material is not included in the article's Creative Commons licence and your intended use is not permitted by statutory regulation or exceeds the permitted use, you will need to obtain permission directly from the copyright holder. To view a copy of this licence, visit <http://creativecommons.org/licenses/by-nc-nd/4.0/>.

© The Author(s) 2024